A Closed-Form Approximation of the Capacity in Multi-Sector Cells: Application to LTE Tri-Sector Antenna

Vincent Savaux, Isabelle Siaud, Rodolphe Legouable

HAL Id: hal-01436598
https://hal.science/hal-01436598

Submitted on 16 Jan 2017

A Closed-Form Approximation of the Capacity in Multi-Sector Cells: Application to LTE Tri-Sector Antenna

Vincent Savaux, Isabelle Siaud, and Rodolphe Legouable

Abstract

This paper deals with the ergodic capacity in multi-sector cells. Due to the presence of the antenna gain pattern in the expression of the capacity, the latter may be difficult to express analytically. In order to overcome this problem, we propose to approximate the antenna gain pattern by means of a piecewise linear function, which leads to a general closed-form formulation of the capacity. The obtained expression is applicable for any used antenna. The simulations results are performed by using the long term evolution (LTE) TR 36.942 antenna specification, showing that the proposed closed-form capacity almost matches the exact one. In addition, we provide a practical use case of the method, by considering a scenario where the users are clustered within the area covered by the antenna.

Keywords – ergodic capacity, multi-sector antenna, closed-form approximation, LTE

I. INTRODUCTION

The capacity is one of the most useful metric evaluated for the design of communication systems and networks. Authors of [1]–[3] shows that quad-sector cells increases the capacity compared with usual tri-sector cells. In [4]–[6], the capacity is used as the parameter to be optimized for bandwidth and power allocation for spectrum sharing in a cognitive radio context. The capacity of multi-input multi-output (MIMO) systems is investigated in [7], [8] in different channel conditions. More recently, the authors of [9], [10] proposed a review of 3-dimensions channel modeling, i.e. considering azimuthal as well as elevation components. However, in most of the papers dealing with capacity, the geometry of the antenna is not taken into account, and antennas are supposed to be omnidirectional.

In this paper, we derive a closed-form approximation of the capacity for multi-sector cells. To this end, we approximate the antenna gain pattern by means of a piecewise linear function. A series expansion of the logarithm and the truncation of the sum then allows to obtain an approximated closed-form of the capacity. This approach is independent of the considered type of antenna, and can be applied to any system. Furthermore, the approximation remains valid in a large range of signal-to-noise ratio (SNR) values. The theoretical developments are accompanied by various simulations results using the LTE TR 36.942 antenna [11], which show the validity of the proposed

expression of the capacity in multi-sector cells. Besides, the limits of the methods, due to the approximation and the truncation, are scrutinized. Moreover, the results are discussed, and we provide a practical use case where our approach may be very useful.

The rest of the paper is organized as follows: Section II describes the motivation and provides a reminder on the expression of the capacity in multi-sector cells. The developments leading to the general closed-form approximation of the capacity are derived in Section III. Section IV is devoted to the simulations results, and we discuss the proposed approach in Section V. We finally draw our conclusion in Section VI.

II. MOTIVATION

In this section, we describe the system model, and we provide a general expression of the capacity in multi-sector cells, which motivates the proposed closed-form approximation.

A. System Model Description

In this paper, the SNR of a user equipment (UE), which is located at a distance r from the transmit antenna, is defined by the log-distance path loss model as

$$\gamma(\theta) = G_{li}(\theta)\gamma_0\left(\frac{r}{r_0}\right)^{-\alpha}, \tag{1}$$

where γ_0 is the SNR measured at distance r_0 from the transmit antenna, and α is the path-loss exponent. It must be noted that the effect of the small scale fading is neglected in (1). Furthermore, a more general model shall involve signal-to-noise plus interference ratio (SINR) instead of SNR. For the matter of simplicity, we conduct our development by using the interference-free model, but the effect of the inter-cell interference (ICI) will be revealed through simulations. It is worth noticing that the direction θ where the UE is located, is taken into account in (1) through the *linear* antenna gain $G_{li}(\theta)$[1]. In most of the papers of the included literature, $G_{li}(\theta)$ is ignored since omnidirectional antennas are considered, therefore $G_{li}(\theta)$ is a constant value for any angular direction θ (see for instance [12], [13]).

In the following, a multi-sector antenna is assumed, and then $G_{li}(\theta)$ varies with θ. Fig. 1 depicts the usual solutions proposed by the antennas manufacturers, namely tri-sector, quad-sector, and six-sector antennas. More details regarding the multi-sector antennas are provided in [1]–[3]. It must emphasized that, in order to provide the most general results, we do not focus on a specific technology nor antenna gain pattern $G_{li}(\theta)$. Without loss of generality, we assume that the antenna gain $G_{li}(\theta)$ is a periodic function from a sector to another one, and it is an odd function in each sector. Note that this assumption is consistent with the actual deployed technologies [11].

In the proposed model, it is supposed that the UEs are homogeneously distributed in the cell, i.e. the distributions $f_\theta(\theta)$ and $f_r(r)$ of the UEs along the angular θ and the distance r from the antenna, respectively, are uniform.

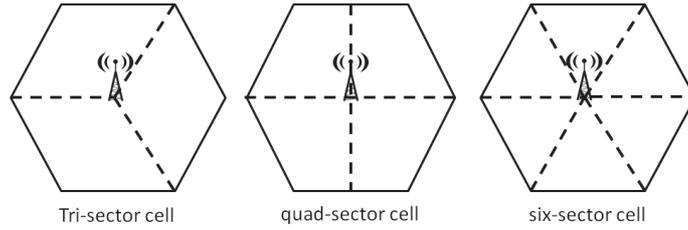[1]The term "linear" means that $G_{li}(\theta)$ is not given in dB.

Fig. 1. Three multi-sector cells, with equal angular divisions.

In the developments provided in Section III, the SNR γ_0 is supposed to be measured at a distance r_0 close to the antenna, in such a way that γ_0 is high valued. Moreover, we denote by R_M the radius of the cell, and K the number of sectors. Besides, in the hereafter the angular values are given in degree.

B. Capacity in Multi-Sector Cells

The average ergodic (or Shannon) capacity in a multi-sector cell, which is denoted by C_e, can be expressed as

$$C_e = \bar{B} \int_0^{R_M} \int_0^{360} \log_2(1 + G_{li}(\theta)\gamma_0 \big(\frac{r}{r_0}\big)^{-\alpha}) f_\theta(\theta) f_r(r) \mathrm{d}\theta \mathrm{d}r, \qquad (2)$$

where $\bar{B}$ is the average bandwidth allocated to the UE. For a clarity purpose, we denote $A(r) = \gamma_0 \big(\frac{r}{r_0}\big)^{-\alpha}$. Since it is supposed that the antenna gain $G_{li}(\theta)$ is the same from a sector to another, and since the uniform distributions are written $f_\theta(\theta) = \frac{1}{360}$ and $f_r(r) = \frac{1}{R_M}$ for any $\theta \in [0, 360]$ and any $r \in [0, R_M]$, (2) reduces to:

$$C_e = \frac{K\bar{B}}{360 R_M} \int_0^{R_M} \int_{\Theta_K} \log_2(1 + G_{li}(\theta)A(r)) \mathrm{d}\theta \mathrm{d}r, \qquad (3)$$

where Θ_K is the angular interval corresponding to one sector (e.g. [0,120] in a tri-sector cell, where $K = 3$). It is worth noticing that the two integrals in (3) are invertible. It can be drawn from (3) that a closed-form of the capacity C_e is very hard to obtain, due to two main reasons:

1) The antenna gain $G_{li}(\theta)$ may not have any analytical expression.
2) The closed-form antiderivative of $\log_2(1 + G_{li}(\theta)A(r))$ with respect to both r and θ variables may not exist in the literature such as [14]. As a matter of fact, the integration of the function with respect to r leads to an hypergeometric function, which is not integrable again with respect to θ.

Based on the points highlighted above, it appears that an approximation of the function to be integrated may be required in order to obtain a non-integral form of C_e. This is proposed in next Section.

III. GENERAL CLOSED-FORM APPROXIMATION OF THE CAPACITY

A. First Approximation of the Capacity

It has been stated in Section II that γ_0 is measured close to the antenna, then $\gamma_0 >> 1$. As a consequence, it can be supposed that $G_{li}(\theta)A(r) > 1$. A necessary and sufficient condition for the latter assumption is provided in

Appendix A. We note $\mathcal{I}$ the integral of $\log_2(1+G_{li}(\theta)\gamma_0\left(\frac{r}{r_0}\right)^{-\alpha})$ with respect to r in (3). Thus, it can be developed by factorizing by $G_{li}(\theta)A(r)$ in the logarithm, and by using the series expansion of $\ln(1+x)$ for $|x| < 1$ (details are provided in Appendix A), such as

$$
\begin{aligned}
\mathcal{I} &= \int_0^{R_M} \log_2(1 + G_{li}(\theta)A(r))\mathrm{d}r \\
&= \frac{1}{\ln(2)} \int_0^{R_M} \ln(G_{li}(\theta)A(r)) + \ln\left(1 + \frac{1}{G_{li}(\theta)A(r)}\right)\mathrm{d}r \\
&= \frac{R_M}{\ln(2)}\left(\ln\left(G_{li}(\theta)A(R_M)\right) + \alpha\right) + \sum_{p=1}^{+\infty} \frac{(-1)^{p+1}R_M^{\alpha p+1}}{\ln(2)G_{li}^p(\theta)\gamma_0^p r_0^{\alpha p}p(\alpha p+1)}.
\end{aligned}
\tag{4}
$$

Due to the presence of γ_0^p in the denominator of the series in (4), the latter converges very fast, and we can limit to P the number of terms in the sum. We denote by $\tilde{\mathcal{I}}$ the approximation of $\mathcal{I}$ using the truncation of the series. The convergence of the terms of the series is discussed in Section IV. Therefore, $\tilde{\mathcal{I}}$ can be substituted into (3), which leads to the first approximation of the capacity. However, due to the presence of $G_{li}(\theta)$ in (4) (and therefore in $\tilde{\mathcal{I}}$), the first drawback, highlighted in Section II, remains.

B. General Approximation of the Capacity

In order to provide a general approximation of the capacity C_e in (3), independently of the analytic expression of the used antenna gain pattern, we propose to approximate $G_{li}(\theta)$ by means of a piecewise linear function denoted by $g(\theta)$, such as illustrated in Fig. 2. The function $g(\theta)$ can be seen as the concatenation of n functions $g_i(\theta) = a_i\theta+b_i$, with $i = [\![1,n]\!]$, and where:

$$
\begin{aligned}
a_i &= \frac{G_{li}(\theta_i) - G_{li}(\theta_{i-1})}{\theta_i - \theta_{i-1}}, \\
b_i &= G_{li}(\theta_i) - a_i\theta_i \\
&= G_{li}(\theta_{i-1}) - a_i\theta_{i-1}
\end{aligned}
\tag{5}
$$

and $\theta_i = \frac{i}{n}\theta$. Thus, the interval Θ_K defined in (3) can now be rewritten as $\Theta_K = [\theta_0, \theta_n]$.

One can then approximate C_e by $\tilde{C}_e$ where:

$$
\tilde{C}_e = \frac{K\bar{B}}{360R_M} \int_0^{R_M} \sum_{i=1}^n \int_{\theta_{i-1}}^{\theta_i} \log_2(1 + g_i(\theta)A(r))\mathrm{d}\theta\mathrm{d}r.
\tag{6}
$$

Furthermore, the substitution of $\tilde{\mathcal{I}}$ into (6), and mathematical developments provided in Appendix B, allow us to obtain a general closed-form approximation of the capacity:

$$
\tilde{C}_e = \frac{K\bar{B}}{360R_M}\left[\sum_{i=1}^n\left(\mathcal{Q}_i(\theta_i) + \mathcal{R}_i(\theta_i) - \mathcal{Q}_i(\theta_{i-1}) + \mathcal{R}_i(\theta_{i-1})\right) + \left(\alpha - 1 + \ln(A(R_M))\right)(\theta_n - \theta_0)\right],
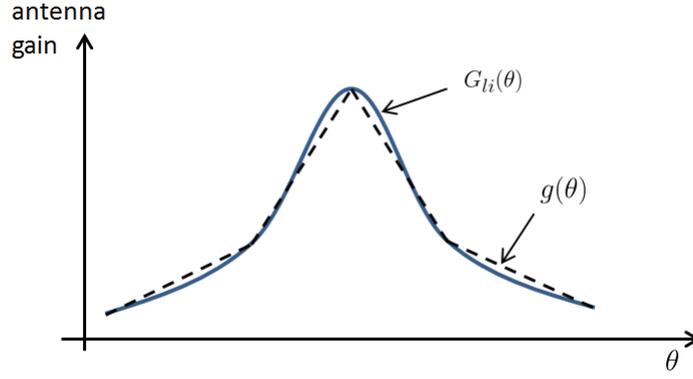\tag{7}
$$

Fig. 2. Antenna gain $G_{li}(\theta)$, and its piecewise linear approximation $g(\theta)$ (dashed line).

where $\mathcal{Q}_i(\theta_i)$ and $\mathcal{R}_i(\theta_i)$ are given, respectively, by:

$$\mathcal{Q}_i(\theta_i) = \frac{R_M}{\ln(2)}\left(\frac{G_{li}(\theta_i)}{a_i}\ln\big(G_{li}(\theta_i)\big)\right), \tag{8}$$

and

$$\mathcal{R}_i(\theta_i) = \frac{R_M^{\alpha+1}\ln(G_{li}(\theta_i))}{\ln(2)a_i\gamma_0 r_0^{\alpha}(\alpha+1)} + \sum_{p=2}^{P}\frac{(-1)^{p+1}R_M^{\alpha p+1}}{\ln(2)G_{li}^{p-1}(\theta_i)a_i(1-p)\gamma_0^p r_0^{\alpha p}p(\alpha p+1)}. \tag{9}$$

It can be drawn from (7)-(9) that the proposed general closed-form approximation of the capacity only depends on some values $G_{li}(\theta_i)$. Thus, it does not require the exact analytical expression $G_{li}(\theta)$, and $\tilde{C}_e$ could even be assessed from an antenna gain pattern defined by a look up table.

IV. NUMERICAL RESULTS: APPLICATION TO LTE TRI-SECTOR CELL

This section aims to show the accuracy of the analytical results by comparing them with the expected results. In order to validate our results, we use the antenna gain defined in the LTE standard 3GPP TR 36.942 [11], which is expressed (in dB) for $\theta \in [-180, 180]$, as

$$G(\theta) = -\min\left\{12\Big(\frac{\theta}{\theta_{3dB}}\Big)^2, A_m\right\}, \tag{10}$$

where $\theta_{3dB} = 90\sqrt{\frac{3}{5}}$, and $A_m = 20$ dB. Fig. 3 depicts the shape of $G(\theta)$, where one sector corresponds to the interval $[-60, 60]$.

It must be noted that this antenna gain pattern leads to closed-form by using the first approximation. In fact, the substitution of $G_{li}(\theta) = 10^{G(\theta)/10}$ into (4) leads to the following expression:
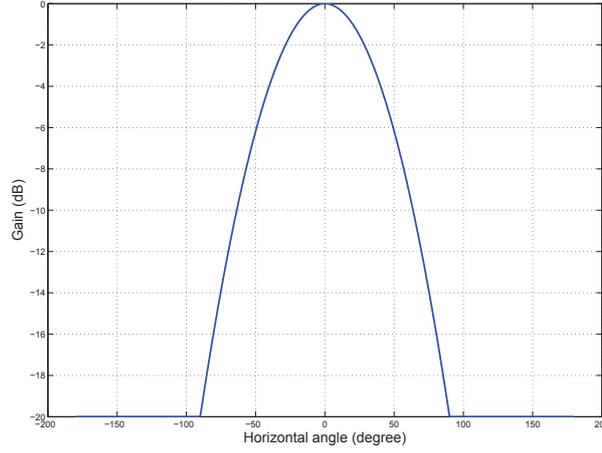
Fig. 3. Gain pattern of the tri-sector antenna 3GPP TR 36.942 [11].

$$C_e = \frac{\bar{B}}{60\ln(2)}\left[\left(60(\alpha + \ln(A(R_M))) - 2\frac{60^3}{5\theta_{3dB}^2}\ln(10)\right)\right.$$
$$\left. + \sum_{i=1}^{+\infty}\frac{(-1)^{p-1}R_M^{\alpha p+1}\sqrt{\pi}\,\text{erfi}\left(\sqrt{\frac{6\ln(10)}{5\theta_{3dB}^2}}60\right)}{\ln(2)\gamma_0^p r_0^{\alpha p} p(\alpha p + 1)2\sqrt{\frac{6\ln(10)}{5\theta_{3dB}^2}}}\right], \tag{11}$$

where erfi(.) is the imaginary error function, which can be written $\text{erfi}(x) = \frac{2}{\sqrt{\pi}}e^{x^2}D(x)$. $D(x)$ is the Dawson's integral, such as described in [14], Chapter 7. The simulations have been performed by using the following parameters: $\gamma_0 = 50$ dB, $r_0 = 5$ m, and $\alpha = 2$. Note that the necessary condition for the convergence of the series, which is given in (17), yields the constraint on the maximum radius of the cell $R_M < 568$ m.

In Fig. 4, we investigate the validity of the truncation of the series thanks to the upper limit P of the sum in $\mathcal{R}_i(\theta_i)$. Thus, Fig. 4 shows the trajectory of the sum in (9) versus the bound limit P. This has been obtained with $n = 20$ intervals, at a distance $r = R_M$, and at $\theta_i = 30°$. It can be observed that the sum converges from $P = 3$ (other simulations revealed that this behavior remains for any r and any θ_i value). This result shows that the truncation is justified, but also that P can be limited to a low value, which reduces the computational complexity of the approximation.

Fig. 5 shows the achieved capacity per unit of frequency[2] versus the radius of the cell, from 5 m to 250 m. The exact value, which is directly obtained by the computation of (3), is compared with the approximation in (11) (referred as "first approx.") and the proposed approximation in (7) (referred "piecewise approx."). It can be seen that the approximated capacity expressions almost match the exact one, although both approximations slightly overestimate the exact value.

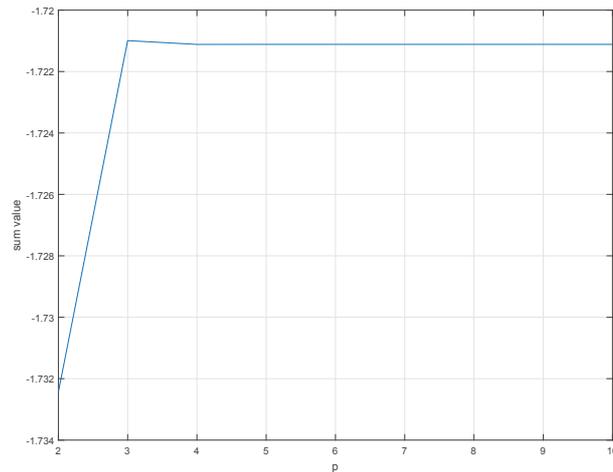[2]Actually, this corresponds to the usual definition of *spectral efficiency*.

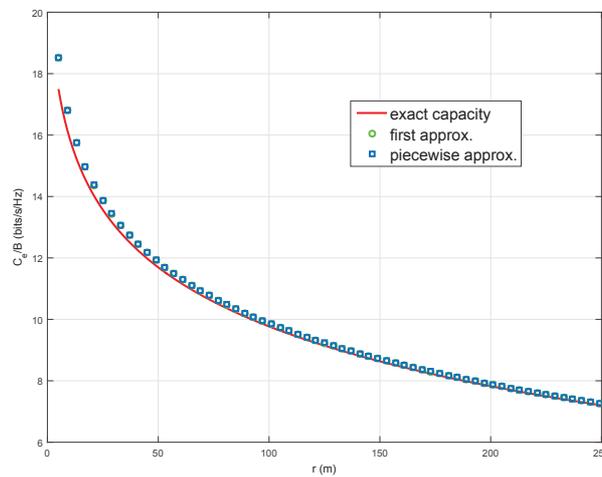Fig. 4. Value of the sum in (9) in function of the limit P.

Fig. 5. Capacity per unit of frequency versus the distance r (m). Comparison of exact and approximated values.

Other series of simulations have been performed in order to show the influence of the number of intervals n on the accuracy of the approximated capacity in (7). Thus, Fig. 6 depicts the error between the exact capacity and the approximated one, namely $|C_e - \tilde{C}_e|$, versus r (m) for different values of $n \in \{4, 8, 20\}$. The results reveal that, for the tested tri-sector antenna, the error is weakly reduced as n increases. This shows that a low value of n allows us to obtain a good approximation. Therefore, in addition with results presented in Fig. 4, we can conclude that the approximated capacity $\tilde{C}_e$ can be assessed with limited complexity.

Fig. 7 shows the capacity per unit of frequency with r from 5 to 1000 m. Thus, the approximations using (11) and the proposed one in (7) are tested beyond the limit of validity of the series expansion of $r = 568$ m. The exact capacity is plotted as reference. Results in Fig. 7 reveal that the approximations indeed hold at $r = 568$ m, as the approximated capacity values match the exact one. Furthermore, it can also be noticed that these approximations
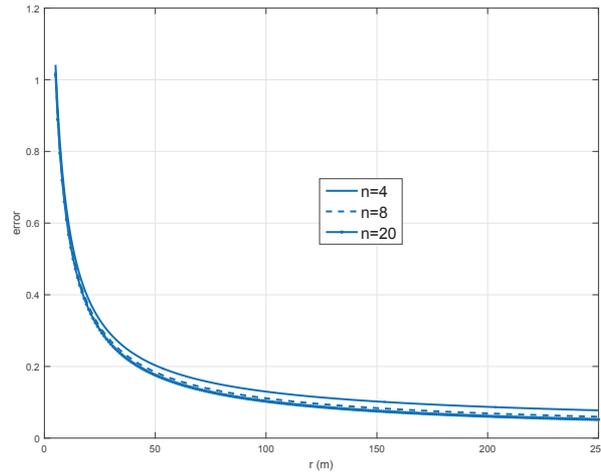
Fig. 6. Error $|C_e - \tilde{C}_e|$ versus r (m) for different values of n.

are still valid up to a limit equal to 750 m. However, it must be emphasized that these results have been obtained with an arbitrary fixed SNR $\gamma = 50$ dB, which might be largely underestimated. Thus, this limit of validity for the approximation may depend on the transmit power of the antenna, which also depends on the considered system.
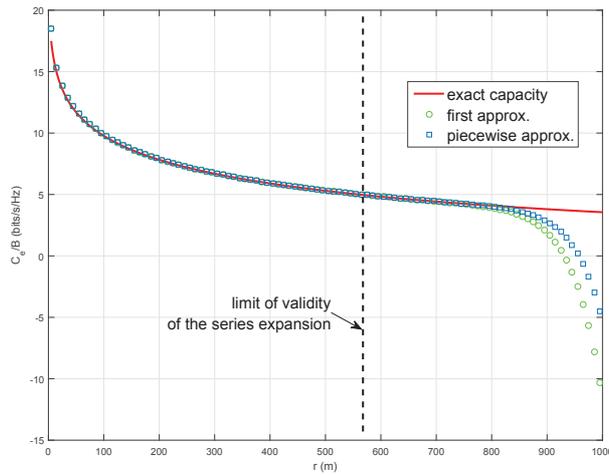

Fig. 7. Capacity per unit of frequency versus the distance r (m) in the limit case where the condition (17) is not respected.

In Fig. 8, we show the cumulative distribution function (cdf) of the capacity in LTE tri-sector cells. The results have been obtained thanks to the Vienna LTE-advanced system link simulator (SLS), which is described in [15], [16]. In order to show the effect of the ICI on the capacity, we compare two scenarios: the no-ICI case where a unique cell is considered, and the ICI case where the capacity is calculated in a cell surrounded by two *rings* of interfering cells. In the latter scenario, which correspond to a more realistic use case, the distance between eNodeBs is set equal to 1000 m. The base stations transmit with a power of 46 dBm, and 60 UEs are distributed in the cell,

namely 20 UEs per sector. In each sector, a bandwidth of 20 MHz (i.e. 100 resource blocks) is allocated to the UEs using the round robin scheduler, and considering a single-input single-output (SISO) mode.
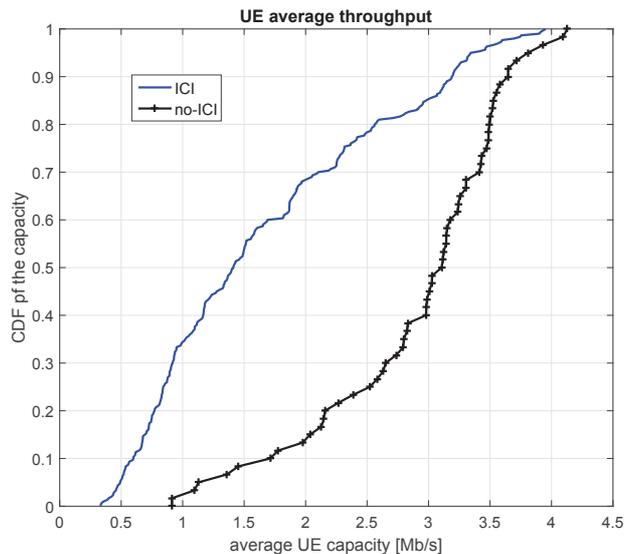

Fig. 8. Effect of ICI on the cumulative distribution function of the capacity.

It can be observed in Fig. 8 that the probability to obtain a weaker capacity value is higher for the ICI than the no-ICI case, which reflects the damaging effect of ICI on the performance of the LTE system. For instance, the value x such that $\mathbb{P}(\text{capacity} \leq x) = 0.5$ is equal to 1.4 and 3.1 MHz in the ICI and no-ICI cases, respectively. However, the more realistic scenario where SINR is used instead of SNR in (1) do not lead to tractable analytical results, and software such as the Vienna SLS is mandatory in order to show the performance of the system.

V. DISCUSSION

In the previous sections, a closed-form approximation of the achievable capacity in multi-sector cells has been proposed. The advantage of the formulation is that it does not depend on the used technology (number of sectors, antenna gain pattern). It has been shown that this approximation match the exact capacity within the predefined limit, and it can be assessed with limited computational cost. However, the developments have been undertaken by considering the capacity in the whole cell. As a consequence, one could discuss the usefulness of the analysis, since a closed-form of the capacity in the cell could be obtained with much more limited complexity.

In fact, let consider an omnidirectional antenna with constant gain β. This β value can be set in order to obtain the same average gain per unit of angle, i.e.:

$$\beta = \frac{K}{360} \int_{\Theta_K} G_{li}(\theta)\mathrm{d}\theta. \tag{12}$$

Then, the capacity in the whole cell can be equivalently calculated by using the omnidirectional antenna with gain β instead of the multi-sector antenna in (3):

$$C_e = \frac{K\bar{B}}{360R_M} \int_0^{R_M} \log_2(1 + A(r))\mathrm{d}r, \tag{13}$$

where $A(r) = \beta\gamma_0\left(\frac{r}{r_0}\right)^{-\alpha}$. This integral can be straightforwardly assessed by using the same approximations as given in this paper. Fig. 9 compares the achieved capacity per unit of frequency versus the distance r (m) for multi-sector antenna and omnidirectional antenna. It can be observed that the value obtained in (13) almost match that obtained by using (3).
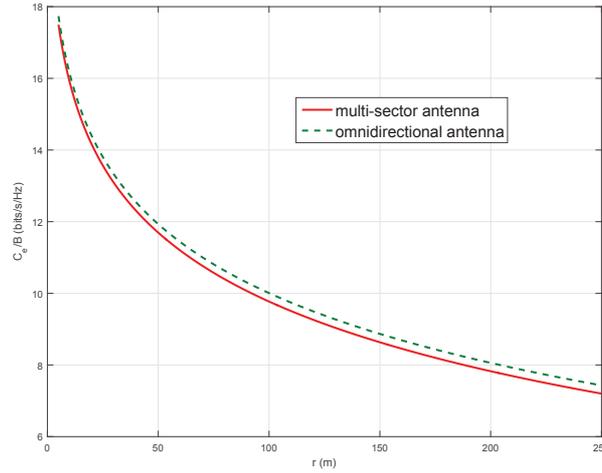

Fig. 9. Capacity per unit of frequency versus the distance r (m): comparison of multi-sector antenna with omnidirectional antenna.

Although (13) shows that the capacity in multi-sector cells can be reduced to the capacity using an equivalent cell with omnidirectional antenna, the proposed approximation may be useful in other practical cases. Thus, let consider clusters of UEs in the multi-sector cell, instead of homogeneously distributed UEs, such as illustrated in Fig. 10, where C_1, C_2, and C_3 are three clusters of UEs. This may correspond, for instance, to the use case of hamlets in a rural area. The goal is then to maximize the overall capacity of the UEs in the clusters, according to the "direction" of the antenna, which is defined as the angle ϕ between an arbitrary axis x and the edge of a sector.

In this use case, it appears that the analysis of the capacity in tri-sector cell is mandatory, since the omnidirectional antenna features a rotational invariance and therefore would lead to the same result for any ϕ value. On the contrary, the proposed piecewise approximation fits such an optimization problem since the gain of the antenna can be substituted by a linear approximation in each angular interval defined by the edges of the cluster: see δ_1, δ_2, and δ_3 on Fig. 10. Therefore, the problem can be formalized as a constrained optimization (three clusters are considered such as illustrated in Fig. 10):

$$\max_{\phi}\left(\tilde{C}_e(C_1,\phi) + \tilde{C}_e(C_2,\phi) + \tilde{C}_e(C_3,\phi)\right) \tag{14}$$
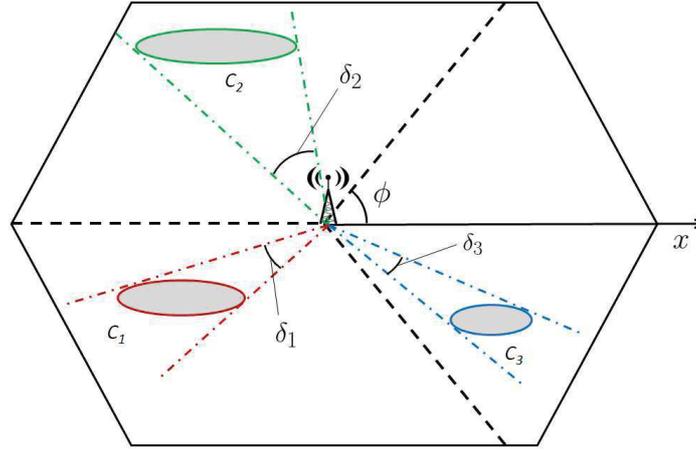
$$\text{subject to } \Omega, \tag{15}$$

Fig. 10. Tri-sector cell with clustered UEs.

where $\tilde{C}_e(C_i, \phi)$ is the approximated capacity in cluster i, and Ω is a set of constraints to be defined. An example of constraint consists in setting a minimum capacity to be achieved in each cluster, namely:

$$\Omega = \begin{cases} \tilde{C}_e(C_1, \phi) \geq C_1^t \\ \tilde{C}_e(C_2, \phi) \geq C_2^t \\ \tilde{C}_e(C_3, \phi) \geq C_3^t \end{cases} \tag{16}$$

where C_i^t are target capacities.

VI. CONCLUSION

In this paper, we presented a general closed-form approximation of the ergodic capacity in multi-sector cells. In fact, the inclusion of the antenna gain pattern in the formulation of the capacity may lead to non-closed expressions. The method consists in approximating the antenna gain thanks to a piecewise linear function. The advantage of the proposed approach lies in its independence of the design of the antenna, such as the number of sectors, as well as the gain pattern. The proposed approximation of the capacity has been validated through simulations, where it is applied to the tri-sector antenna TR 36.942 defined in the 3GPP standard. Simulations results revealed that the proposed capacity almost matches the exact one, converges in a large range of cell radius, and requires only few pieces of linear functions. Furthermore, the method has been discussed, and a practical application of the closed-form approximation has been proposed. Further work aims to extend the analysis to the case of more realistic channel models.

APPENDIX

A. Obtaining the First Approximation

The series expansion of the logarithm in (4) holds if $G_{li}(\theta)A(r) > 1$, for any $\theta \in [0, 360]$ and any $r \in [0, R_M]$. Therefore, given a fixed SNR, we can deduce a necessary and sufficient condition on R_M in order to derive the series expansion of the logarithm:

$$G_{li}(\theta)A(r) > \min_{\theta}(G_{li}(\theta))A(R_M) > 1$$

$$\Leftrightarrow R_M < r_0\big(\gamma_0 \min_{\theta}(G_{li}(\theta))\big)^{1/\alpha}. \tag{17}$$

The series expansion of $\ln(1 + x)$ for $|x| < 1$ is:

$$\ln(1 + x) = \sum_{p=0}^{+\infty} \frac{(-1)^{p-1}x^p}{p}. \tag{18}$$

If (17) holds, then the second term in (4) yields

$$\int_0^{R_M} \ln\left(1 + \frac{1}{G_{li}(\theta)A(r)}\right)dr = \int_0^{R_M} \sum_{p=1}^{+\infty} \frac{(-1)^{p+1}r^{\alpha p}}{\ln(2)G_{li}^p(\theta)\gamma_0^p r_0^{\alpha p} p}dr$$

$$= \sum_{p=1}^{+\infty} \frac{(-1)^{p+1}R_M^{\alpha p+1}}{\ln(2)G_{li}^p(\theta)\gamma_0^p r_0^{\alpha p} p(\alpha p + 1)}, \tag{19}$$

which leads to the expression of $\mathcal{I}$ in (4).

B. Obtaining the General Closed-Form Approximation

We carry out in (6) the same development as in (4) by using a truncated sum, which leads to

$$\tilde{C}_e = \frac{K\bar{B}}{360R_M} \int_0^{R_M} \sum_{i=1}^{n} \int_{\theta_{i-1}}^{\theta_i} \log_2(1 + g_i(\theta)A(r))d\theta dr$$

$$= \frac{K\bar{B}}{360R_M} \sum_{i=1}^{n} \left[\underbrace{\int_{\theta_{i-1}}^{\theta_i} \frac{R_M}{\ln(2)}\big(\ln\big(G_{li}(\theta)A(R_M)\big) + \alpha\big)d\theta}_{\mathcal{J}_1} \right.$$

$$\left. + \underbrace{\int_{\theta_{i-1}}^{\theta_i} \sum_{p=1}^{P} \frac{(-1)^{p+1}R_M^{\alpha p+1}}{\ln(2)G_{li}^p(\theta)\gamma_0^p r_0^{\alpha p} p(\alpha p + 1)}d\theta}_{\mathcal{J}_2} \right]. \tag{20}$$

We can now develop $\mathcal{J}_1$ and $\mathcal{J}_2$ independently:

$$\mathcal{J}_1 = \int_{\theta_{i-1}}^{\theta_i} \frac{R_M}{\ln(2)} \big(\ln\big((a_i\theta + b_i)A(R_M)\big) + \alpha \big) \mathrm{d}\theta$$

$$= \frac{R_M}{\ln(2)} \Big(\ln(a_i\theta_i + b_i)(\frac{b_i}{a_i} + \theta_i) + \theta_i(\alpha - 1 + \ln(A(R_M)))$$

$$- \ln(a_i\theta_{i-1} + b_i)(\frac{b_i}{a_i} + \theta_{i-1}) + \theta_{i-1}(\alpha - 1 + \ln(A(R_M))) \Big). \tag{21}$$

Since $G_{li}(\theta_i) = a_i\theta_i + b_i$, we recognize $\mathcal{Q}_i(\theta_i) = \frac{R_M}{\ln(2)} \ln(a_i\theta_i + b_i)(\frac{b_i}{a_i} + \theta_i)$. The development of $\mathcal{J}_2$ is given by

$$\mathcal{J}_2 = \int_{\theta_{i-1}}^{\theta_i} \frac{R_M^{\alpha+1}}{\ln(2)G_{li}(\theta)\gamma_0 r_0^\alpha(\alpha + 1)} + \sum_{p=2}^{P} \frac{(-1)^{p+1}R_M^{\alpha p+1}}{\ln(2)G_{li}^p(\theta)\gamma_0^p r_0^{\alpha p} p(\alpha p + 1)} \mathrm{d}\theta$$

$$= \frac{R_M^{\alpha+1}\ln(a_i\theta_i + b_i)}{\ln(2)a_i\gamma_0 r_0^\alpha(\alpha + 1)} + \sum_{p=2}^{P} \frac{(-1)^{p+1}R_M^{\alpha p+1}}{\ln(2)(a_i\theta_i + b_i)^{p-1}a_i(1 - p)\gamma_0^p r_0^{\alpha p} p(\alpha p + 1)}$$

$$- \frac{R_M^{\alpha+1}\ln(a_i\theta_{i-1} + b_i)}{\ln(2)a_i\gamma_0 r_0^\alpha(\alpha + 1)} - \sum_{p=2}^{P} \frac{(-1)^{p+1}R_M^{\alpha p+1}}{\ln(2)(a_i\theta_{i-1} + b_i)^{p-1}a_i(1 - p)\gamma_0^p r_0^{\alpha p} p(\alpha p + 1)}, \tag{22}$$

where one can recognize $\mathcal{R}_i(\theta_i)$.

REFERENCES

[1] L. C. Wang and K. K. Leung, "Performance enhancement by narrow-beam quad-sector cell and interleaved channel assignment in wireless networks," in *proc. of globecom'99*, vol. 5, Rio de Janeiro, Brazil, December 1999, pp. 2719 – 2724.

[2] ——, "A high-capacity wireless network by quad-sector cell and interleaved channel assignment," *IEEE Journal on Selected Areas in Communications*, vol. 18, no. 3, pp. 472 – 480, March 2000.

[3] O. W. Ata, H. Seki, and A. Paulraj, "Capacity enhancement in quad-sector cell architecture with interleaved channel and polarization assignments," in *proc. of ICC'01*, vol. 7, Helsinki, Finland, June 2001, pp. 2317 – 2321.

[4] L. Musavian and S. Aissa, "Capacity and power allocation for spectrum-sharing communications in fading channels," *IEEE Transactions on Wireless Communications*, vol. 8, no. 1, pp. 1536 – 1276, January 2009.

[5] X. Kang, Y.-C. Liang, A. Nallanathan, and R. Garg, H. K. Zhang, "Optimal power allocation for fading channels in cognitive radio networks: Ergodic capacity and outage capacity," *IEEE Transactions on Wireless Communications*, vol. 8, no. 2, pp. 940 – 950, Februray 2009.

[6] X. Gong, S. A. Vorobyov, and C. Tellambura, "Optimal Bandwidth and Power Allocation for Sum Ergodic Capacity Under Fading Channels in Cognitive Radio Networks," *IEEE Transactions on Signal Processing*, vol. 59, no. 4, pp. 1814 – 1826, April 2011.

[7] M. Matthaiou, N. D. Chatzidiamantis, and G. K. Karagiannidis, "A New Lower Bound on the Ergodic Capacity of Distributed MIMO Systems," *IEEE Signal Processing Letters*, vol. 18, no. 4, pp. 227 – 230, April 2011.

[8] H. Shin and J. H. Lee, "Closed-form Formulas for Ergodic Capacity of MIMO Rayleigh Fading Channels," in *proc. of ICC'03*, vol. 5, Anchorage, Alaska, May 2003, pp. 2996 – 3000.

[9] A. Kammoun, H. Khanfir, Z. Altman, M. Debbah, and M. Kamoun, "Preliminary Results on 3D Channel Modeling: From Theory to Standardization," *IEEE Transactions on Selected Areas in Communications*, vol. 32, no. 6, pp. 1219 – 1229, June 2014.

[10] J. Zhang, C. Pan, F. Pei, G. Liu, and X. Cheng, "Three-dimensional fading channel models: A survey of elevation angle research," *IEEE Communications Magazine*, vol. 52, no. 6, pp. 218 – 226, June 2014.

[11] ETSI, "LTE; Evolved Universal Terrestrial Radio Access (E-UTRA); Radio Frequency (RF) system scenarios (3GPP TR 36.942 version 8.2.0 Release 8)," ETSI, Tech. Rep., 2009.

[12] A. Goldsmith, "Wireless Communications," *Standford University*, 2004.

[13] S. Choudhury and J. D. Gibson, "Ergodic capacity, outage capacity, and information transmission over Rayleigh fading channels," in *proc. of the Information Theory and Applications Workshop*, January 2007.

[14] M. Abramowitz and I. Stegun, *Handbook of Mathematical Functions with Formulas, Graphs, and Mathematical Tables*. Ney York: Dover, 1970, ch. 6.

[15] C. Mehlführer, J. C. Ikuno, M. Šimko, S. Schwarz, M. Wrulich, and M. Rupp, "The Vienna LTE simulators - Enabling reproducibility in wireless communications research," *EURASIP Journal on Applied Signal Processing*, vol. 2011, no. 29, pp. 1 − 14, December 2011.

[16] M. Rupp, S. Schwarz, and M. Taranetz, *The Vienna LTE-Advanced Simulators*. Singapore: Springer, 2016.